Near-infrared color vs launch date: an analysis of 20 years of space weathering effects on the Boeing 376 spacecraft

James Frith
University of Texas El Paso
Jacobs JETS Contract, NASA Johnson Space Center
2224 Bay Area Blvd., Houston, TX 77058
Phillip Anz-Meador
Jacobs, NASA Johnson Space Center, 2224 Bay Area Blvd., Houston, TX 77058
Heather Cowardin
University of Texas El Paso
Jacobs JETS Contract, NASA Johnson Space Center
2224 Bay Area Blvd., Houston, TX 77058
Brent Buckalew
Jacobs, NASA Johnson Space Center, 2224 Bay Area Blvd., Houston, TX 77058
Susan Lederer
NASA Johnson Space Center, 2101 NASA Parkway, Houston TX 77058

ABSTRACT

The Boeing HS-376 spin stabilized spacecraft was a popular design that was launched continuously into geosynchronous orbit starting in 1980, with the last launch occurring in 2003. Over 50 of the HS-376 buses were produced to fulfill a variety of different communication missions for countries all over the world. The design of the bus is easily approximated as a telescoping cylinder that is covered with solar cells and an Earth-facing antenna that is despun at the top of the cylinder.

The similarity in design and the number of spacecraft launched over a long period of time make the HS-376 a prime target for studying the effects of solar weathering on solar panels as a function of time. A selection of primarily non-operational HS-376 spacecraft launched over a 20-year time period were observed using the United Kingdom Infrared Telescope on Mauna Kea and multi-band, near-infrared photometry produced. Each spacecraft was observed for an entire night cycling through ZYJHK filters and time-varying colors produced to compare near-infrared color as a function of launch date. The resulting analysis shown here may help in the future to set launch date constraints on the parent object of unidentified debris objects or other unknown spacecraft.

1. INTRODUCTION

The Hughes/Boeing HS-376/BSS-376 spacecraft were launched prolifically from 1980 to 2003, providing communication services for a multitude of countries. A simple and effective design allowed it to be quickly assembled and launched, which also added to its popularity. The design consisted of a roughly 2-meter diameter spin-stabilized cylinder covered primarily in solar cells with a thermal radiator collar and a despun, Earth-facing antenna at the top. After being deployed, the spacecraft extended approximately 6.5 - 7 m.

Ultimately, as power needs increased, the design proved an evolutionary dead-end. A “skirt,” which consisted of a concentric structure with more solar cells that could be deployed downward after launch, was implemented to double the length and add additional solar cell surface area. These spacecraft held the designation HS-376HP (high power). Additionally, the HS-376W (wide) increased the surface area by enlarging the diameter of the bus. But in the end, adding extra solar panels to increase the wingspan of a three-axis stabilized spacecraft proved a much simpler way to increase overall power output and the bus was retired.

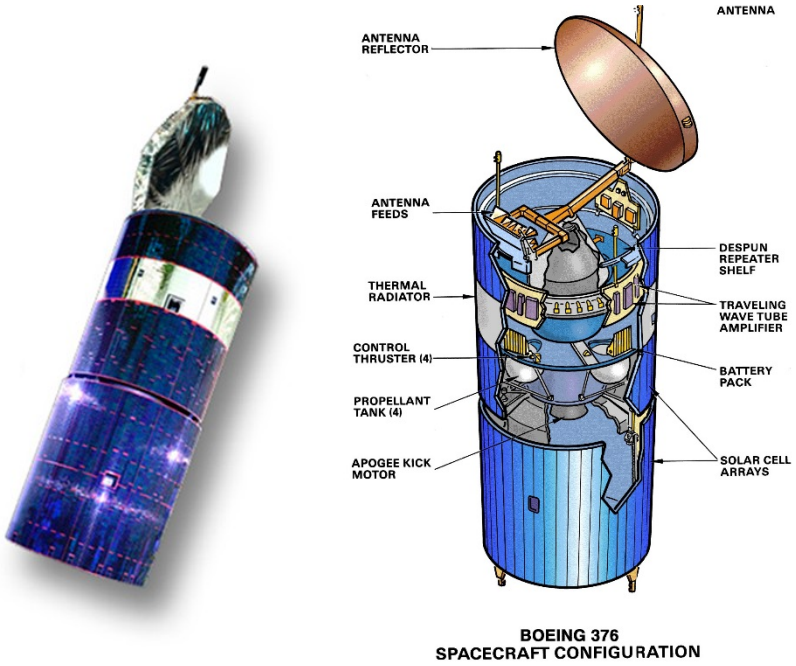

Fig. 1. Many dozen HS-376 models, all with similar design, were launched continuously from 1980 to 2003 (Images credited to Boeing)

Due to their popularity and ubiquitous presence in or near-geosynchronous belt (GEO) orbits, understanding their reflective properties is useful both to monitor the population as a whole and to use information gained as a potential corollary to other spacecraft that have surfaces primarily covered by solar panels. Space weathering of solar cells is not well characterized and understanding the expected changes in the absorption or reflective properties over time could provide insight into the material properties of uncatalogued debris.

Solar cells, by design, absorb light in the visible region of the spectrum but some evidence has suggested they are more reflective at redder wavelengths. Specifically, in 2009, two HS-376 spacecraft, one launched in 1981 (SBS-2) and one in 1994 (Galaxy 1R), were observed using the Infrared Telescope Facility (IRTF) by Abercromby, et al. Low resolution spectra were obtained using the SpecX instrument, which covered a wavelength range from roughly 0.6 - 2.6 μm. Their results are seen in Fig. 2. These spectra have been calibrated using solar-analogue stars to account for the decreased emission of the Sun at longer wavelengths and are not entirely representative of the integrated photometric values one could expect to observe. However, a sharp increase in reflectivity of these spacecraft occurs for wavelengths greater than 1μm.

As a result, due to the object's increased albedo at those wavelengths, orbital debris surveys using the near-infrared (NIR) (1 - 2.5 μm) may provide the ability to see smaller objects of particular material-type. Understanding of the NIR reflective properties of known, on-orbit material-types is needed before any identification of uncharacterized debris objects can be made using this technique. This work, therefore, focuses on using the simple geometric design and the abundant on-orbit availability of the HS-376 bus to examine how this population's solar cells have been affected over 20 years in a deep space environment.

2. OBSERVATIONS

The NASA Orbital Debris Office acquired 35% of the observing time of the United Kingdom Infared Telescope (UKIRT) in 2014 and 2015 to add to its ground based assets for studying the orbital debris

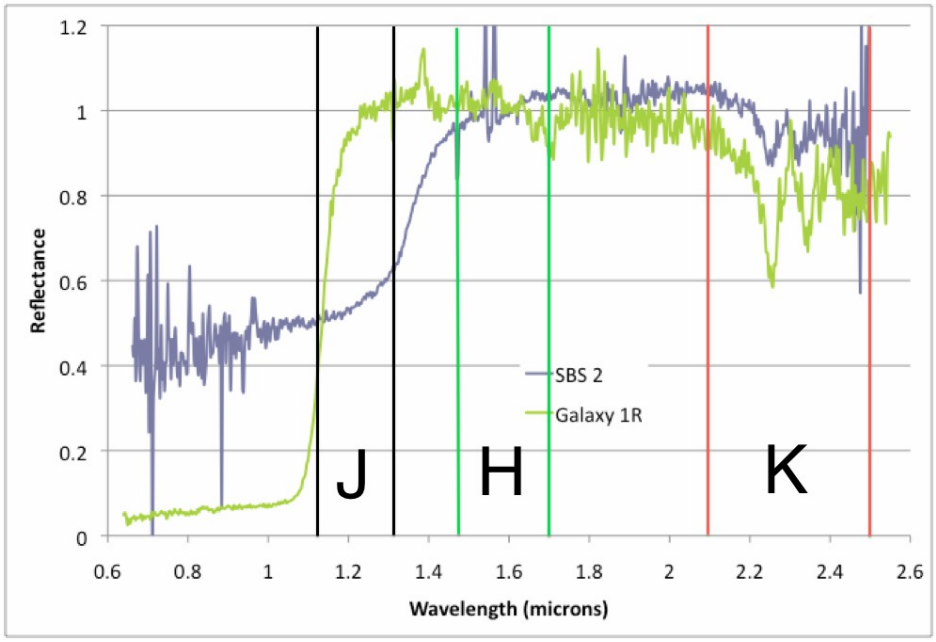

Fig. 2. IRTF spectral observations, using the SpeX instrument, showing the observed reflectance as a function of wavelength of two HS-376 buses produced by Abercromby et al [3]. The approximate NIR band pass sensitivities available using UKIRT have been added (JHK). A large spike in the reflectance of the two spectra can be seen for wavelengths greater than μm though this spike occurs at different wavelengths for each spacecraft.
SBS-2 was launched in 1981 and Galaxy 1R was launched in 1994.

environment. UKIRT's Wide Field Camera (WFCAM) was used for these observations that provide NIR photometry across approximately 0.9 - 2.4 μm (see Fig. 3). The focal plane consists of four separated Rockwell Hawaii-II (mercury cadmium telluride [HgCdTe] 2048 x 2048) arrays that have traditionally been used for sidereal surveys by offsetting four consecutive observations such that the four observations cover a 0.75 square degree field. More information about the WFCAM instrument and data pipeline can be found in [1] and [2].

In November of 2014, 10 nights centered around the new Moon were dedicated towards obtaining NIR photometry of a selection of primarily non-active HS-376 spacecraft. The target selection criteria was optimized to observe objects with a similar bus type that covered a wide range of launch years and that had good visibility over Hawai'i during the observing run. All were HS-376 buses except for one HS-376HP, which was also observed (see Table 1).

The observing technique was designed to obtain the maximum amount of phase angle coverage possible for every target and to cycle through all available filters continuously. The objects were rate tracked such that the stars were streaks and the spacecraft were point sources with sidereal images taken before and after each set of filter observations to obtain calibration sources. Two, 5-second exposures were co-added per observation. The objects were visibly acquired by the operator and centered on chip number 3 of the instrument, which has the fewest defects of the four chips (see Fig. 3). In total, eight targets were successfully observed and their light curves can be found in Fig. 4. Two targets only had sparse coverage due to bad weather.

The raw data were collected and transferred to the Cambridge Astronomical Survey Unit (CASU) at the Institute of Astronomy to be put through their pipeline for processing. A text file containing all of the photometrically calibrated point source detections was then produced and transferred to the NASA Johnson Space Center. Photometric uncertainties are ≤ 0.1 magnitudes for each filter.

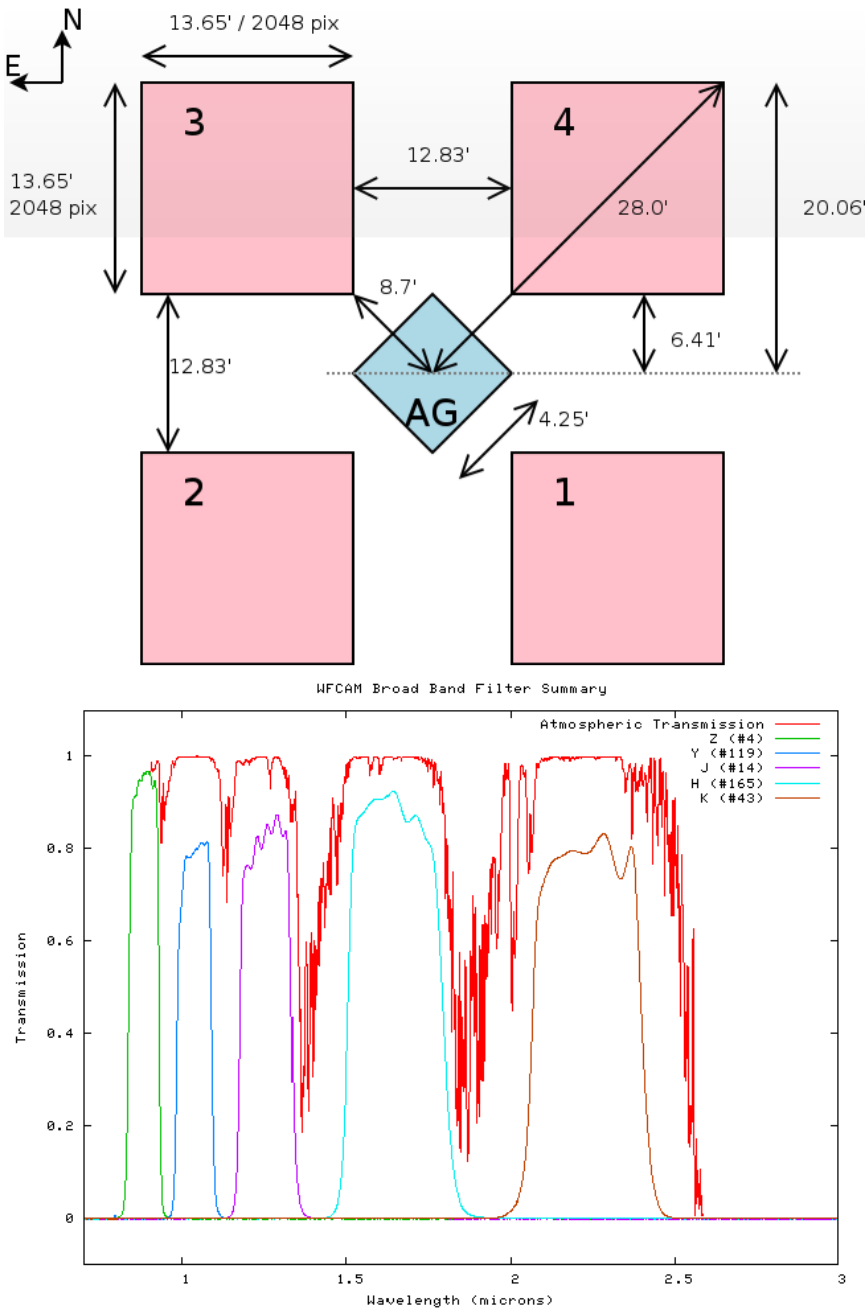

Fig. 3. Upper: Layout of WFCAM's focal plane showing the 4 HgCdTe 2048 x 2048 arrays and the visible auto guider in the center. Lower: Transmission as a function of wavelength for WFCAM's filter set and the atmospheric absorption/transmission at those corresponding wavelengths. All filters were used for these observations.

3. ANALYSIS

CASU has worked extensively with NASA to modify their pipeline to more easily detect rate-tracked man-made objects, but many false detections are still produced due to the noisy nature of the detector. These were weeded out using a combination of magnitude and positional constraints as well as manual inspection of the images. After removing false detections, light curves for each object were produced and can be seen in Fig. 4.

Table 1. Physical properties of the spacecraft observed using WFCAM on UKIRT in November 2014. All bus-types are HS-376 with the exception of ASTRA 3A, which is an HS-376HP.

Int Des	SSN #	Launch Year	Name	Length Deployed	Diameter	On-orbit Mass
1980-091A	12065	1980	SBS 1	6.6 m	2.16 m	540 kg
1983-077A	14234	1983	Telstar 3A	6.84 m	2.16 m	653 kg
1984-113B	15383	1984	ANIK D2	6.84 m	2.16 m	653 kg
1985-109B	16274	1985	MORELOS 2	6.62 m	2.16 m	646.5 kg
1990-034A	20570	1990	Palapa B2R	6.96 m	2.16 m	692 kg
1990-091B	20873	1990	Galaxy 6	6.6 m	2.2 m	709 kg
1994-043A	23185	1994	APSTAR 1	7.5 m	2.2 m	726 kg
2002-015B	27400	2002	ASTRA 3A	7.97 m	2.17 m	908 kg

4. COLOR DETERMINATION

Because of the non-simultaneity of the multi-filter observations, a method was needed to properly compare measurements taken in one filter to the other such that an estimate of the color (J-K, H-Z, etc.) could be achieved. Therefore, a polynomial fit was produced for each filter for every object and points were evaluated along the fit at 5-minute intervals during a given night. The order of the fits varied and was dependent on the number of blocks of observations available for each filter. This effectively smoothed out any time-varying fluctuations in brightness and produced interpolated magnitudes in all filters during the same time period. These fits can also be seen in Fig. 4. For the observations of ASTRA 3A, it was found that no meaningful fit could be achieved using this method due to its highly variable light curve. It was, therefore, not included in later color analyses.

5. DISCUSSION

5.1 Solar Cell Differences

The HS-376 bus helps to restrict shape and material variations one would get from objects with a more complicated geometry, but there are still many variations in color and magnitude that could be caused by various solar cells being used. Four types of solar cells were used during the two decades of manufacturing the HS-376, all produced by Spectrolab and verified by Boeing (obtained via private communication with Boeing).

1. **K4 3/4:** Shallow junction n/p silicon (Si) cell with back surface reflector
2. **K7:** Shallow junction n/p Si cell with back surface field, back surface reflector and textured front surface
3. **Gallium arsenide (GaAs)/Germanium (Ge):** p/n single junction GaAs device grown on Ge substrate
4. **$GaInP_2$/GaAs/Ge:** Dual junction n/p device grown on inactive Ge substrate

All of these solar cell types could also further be combined with several different varieties of cover glass sitting on top of the solar cell. Both of these, obviously, could change the reflective properties as seen from ground observations so further knowledge of the specific design of each spacecraft is needed and is currently being investigated.

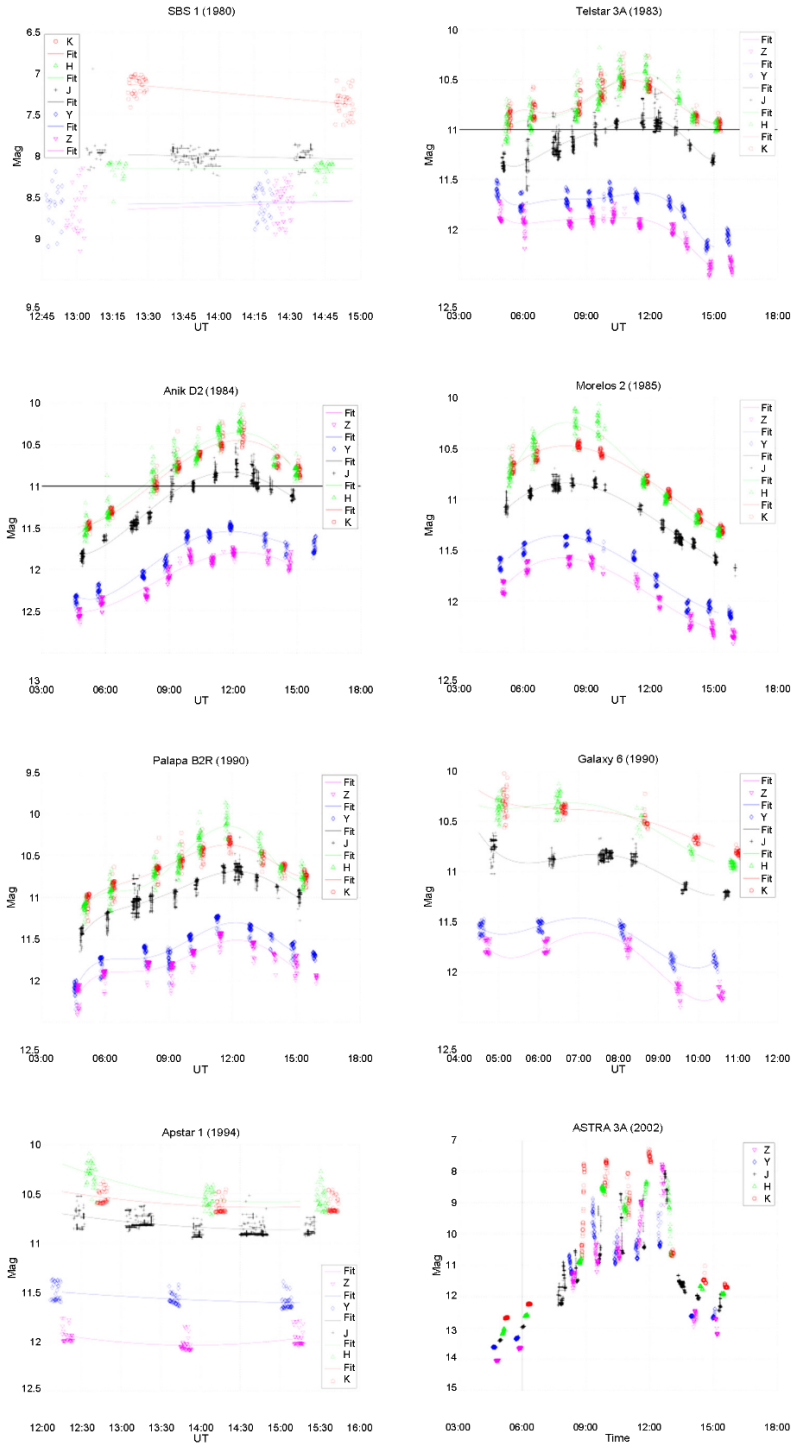

Fig. 4. NIR light curves of the observed objects. All are inactive HS-376 buses with the exception of ASTRA 3A, which is an active HS-376HP. Polynomial fits for each filter are shown as solid lines. SBS-1 (upper left) had limited observations due to incremental weather and was found to be significantly brighter (two to four magnitudes), which may indicate a cross tag or unusual facet of the object being presented during the short duration of observations. Astra 3A was found to be highly variable and no meaningful polynomial fits could be obtained using this method. The highly variable light curve may be due to a periodic glinting surface caused by it still being active/spin-stabilized.

5.2 Object Comparisons

Cross tags and object identification are always a possibility so, as a sanity check, Fig. 5 compares the smoothed J-band light curves as a function of longitudinal phase angle (positive values indicate the Sun is east of the satellite and negative values indicate it is to the west). When looking at the objects in this way, it is readily apparent that at least one of the objects behaves differently than the others. SBS-1 (launched in 1980), though only a very sparse data set, is far brighter than any of the other objects at similar phase angles. The reason for this is not known. This could be a possible cross-tag (the U.S. Strategic Command Space Surveillance Network catalog identifying it incorrectly as SBS-1), but further observations that cover a wider range of time and phase angle would help narrow down why this may be the case.

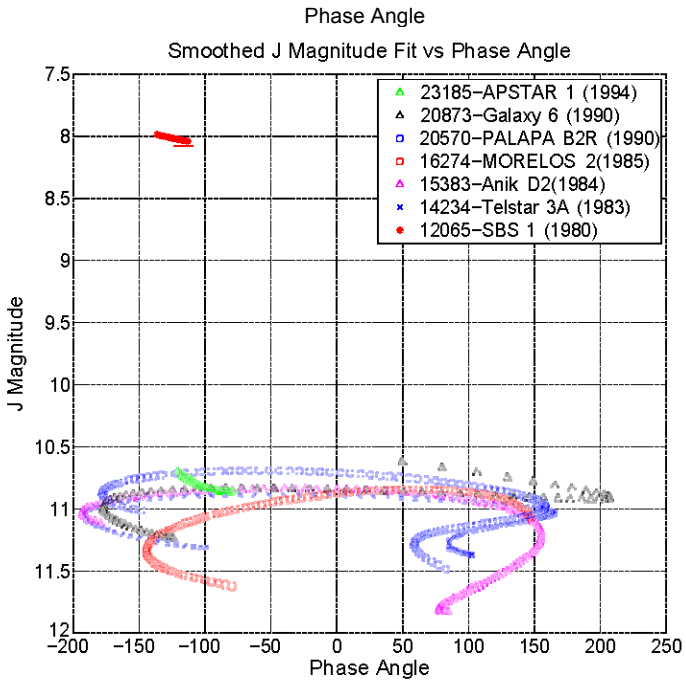

Fig. 5: Smoothed J magnitude versus longitudinal phase angle. The positive values represent the Sun being east of the satellite and the negative values indicate being to the west. All objects observed have a similar spread in J magnitude across phase space except for SBS-1, which is a clear outlier. This may be due to a cross-tag or the surface material being very different from the other objects observed.

Many color indices can be examined with these data, but this work will focus on the NIR colors (J-K, H-K) in order to explore the NIR reflectivity changes found in Abercromby, et al. When examined as a group, there are similarities in variations of J-K across phase angle space but more deviations exist than in Fig. 5. Fig. 6 shows the interpolated J-K and H-K values of all objects observed as a function of phase angle. Interestingly, as the targets approach low phase angles in the J-K plot, most of them pass through or get close to a J-K equal to that of the Sun. This likely is due to receiving a more specular reflective component from the surface material, essentially providing an image of the Sun. This could be a reflection or glint off the thermal radiator collar (see Fig. 1).

The deviation of Galaxy 6 and, to a lesser extent, Palapa B2R, may indicate that they are of dissimilar design than others or that perturbations in their orbits have caused them to present an edge-on cross section potentially exposing different materials. Perhaps coincidentally, both objects were launched in 1990. This deviance can be further examined to determine whether the solar cells used between these two objects differ from other observed objects when additional information on their design specifics is obtained from the manufacturer .

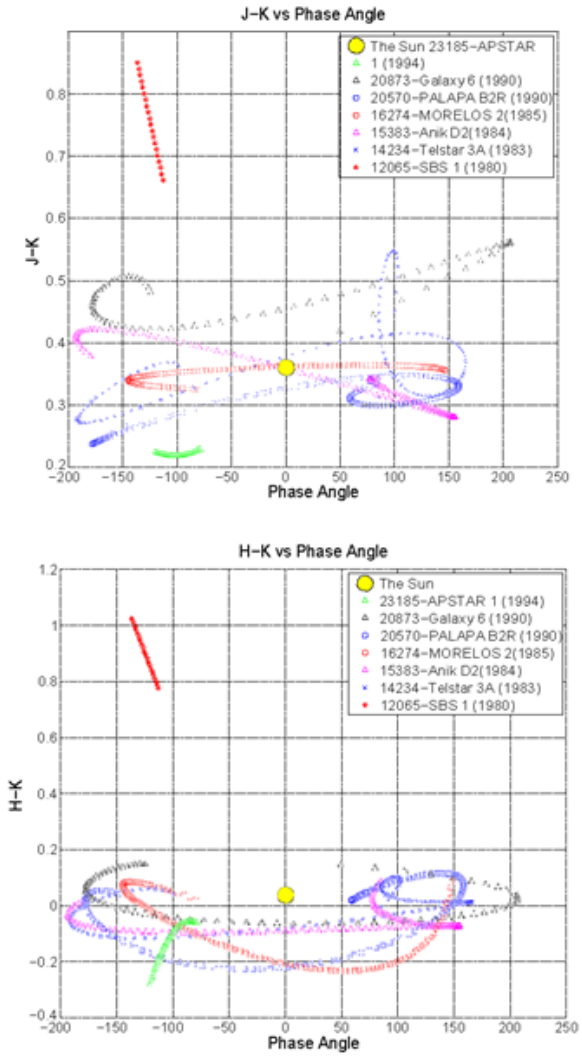

Fig. 6. Interpolated J-K and H-K colors as a function of the solar phase angle of the objects observed. J-K values tend towards solar colors at low phase angles while H-K do not show a similar trend. SBS-1 is still a significant outlier in color space as it is in brightness, as seen in Fig. 4, which may indicate a cross tag.

The H-K values are also interesting, particularly in the way that they differ from the J-K values. The H-K values do not trend towards solar colors as dramatically as they do in the J-K at low phase angles. This may be due to the primary material responsible for the reflection having less of a specular component in the H band. Looking back to the light curves in Fig. 4, the H-band magnitudes vary with respect to the K-band magnitudes much more erratically than the other bands, which may also indicate potential absorption features specific to H band for the observed materials. Further spectral studies of both materials on the ground using the solar cells discussed above, as well as using UKIRT's spectral instruments, are currently on-going and will be presented at a future date.

Finally, in order to better examine how the target's NIR color changes as a function of time on-orbit, the mean J-K and H-K colors for the entire night were calculated for each object and plotted against the object's launch date. These plots can be seen in Fig. 7.

Though this is an obvious simplification, a trend can be seen where objects that have been on-orbit longer have a larger J-K value. This implies a "reddening" (the filter with the longer central wavelength being brighter than the filter with the shorter central wavelength) in their NIR color of the object over time. As in Fig. 6, Galaxy 6 appears to be an exception to this trend for unknown reasons. Its sparse data set and significantly different brightness level imply that

SBS-1 may also be an outlier, so more observations are needed of that object.

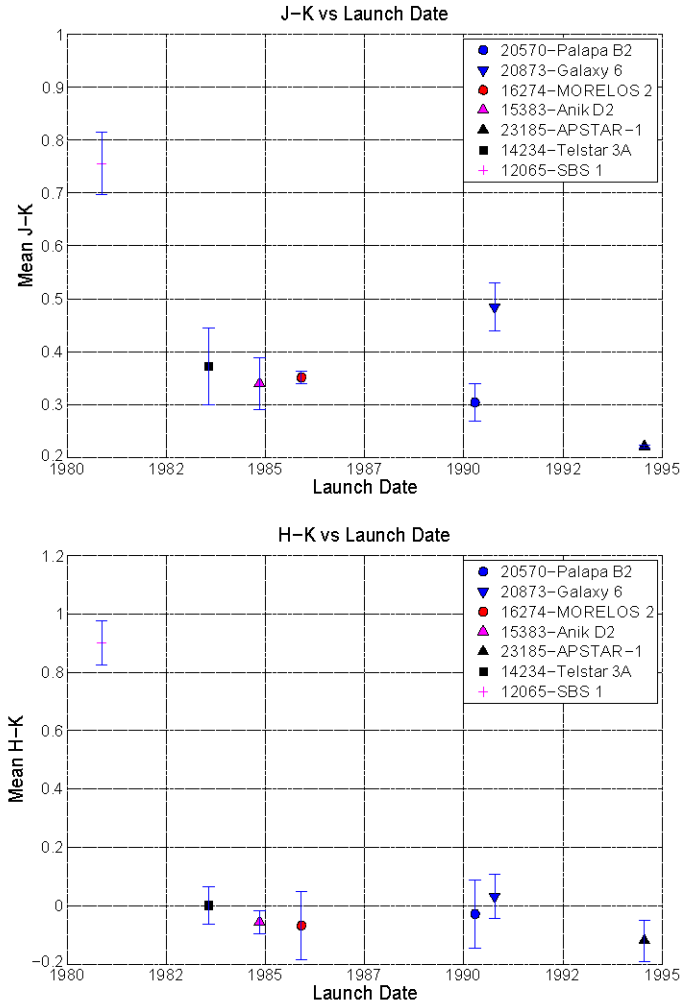

Fig. 7. Mean J-K and H-K values for each object observed over whole observing period (for most objects, one full night). The error bars represent 1σ of the mean. In both colors, a "reddening" trend seems to occur for HS-376s that have been on-orbit longer though Galaxy 6 appears to not hold to this trend. SBS-1 appears to match the trend but was shown earlier to be much brighter than the other buses as well as having a much redder color. This is either a result of a cross tag or very different materials affecting the brightness and the color of this spacecraft.

6. CONCLUSIONS AND FUTURE WORK

Using a subset of our recent UKIRT observations, a possible relationship between observed mean J-K color variations as a function of time on orbit has been identified. However, this relationship is currently plagued by small number statistics. Further data are needed in order to validate the relationship as a possible tool for future debris characterization.

Additional photometric and spectral observations of these and other HS-376 spacecraft have already been obtained but are still being processed to further help clarify the validity of these preliminary conclusions. Of particular importance is to identify the specific solar cell design used for each spacecraft for which data has been obtained. Further comparison to other objects on-orbit that are not of the HS-376 design needs to be implemented if the relationship may apply to other types of spacecraft materials and shapes.

This is a rich data set with many opportunities for specific object characterization including tumble rates, orientation,

and further analysis of specific material properties that were observed. All of this is currently being explored.

7. REFERENCES

1. Casali, M et al. The UKIRT wide-field camera, Astronomy and Astrophysics, Volume 467, Issue 2, May IV 2007, pp.777-784
2. Kendrick, R et al. Orbital Debris Observations with WFCAM, Proceedings of the Advanced Maui Optical and Space Surveillance Technologies Conference 2014
3. Abercromby, K et al. Reflectance Spectra Comparison of Orbital Debris, Intact Spacecraft, and Intact Rocket Bodies in the GEO regime, Proceedings of the Advanced Maui Optical and Space Surveillance Technologies Conference 2009.